Dynamic NMR Spectroscopy of Hyperpolarized ^{129}Xe in Human Brain Analyzed by an Uptake Model

Wolfgang Kilian, Frank Seifert, and Herbert Rinneberg

From the Physikalisch-Technische Bundesanstalt, Berlin, Germany

Published in Magn. Reson. Med. **51**, 843-847 (2004); DOI: 10.1002/mrm.10726

Address correspondence to:
Dr. Wolfgang Kilian
Lab. 8.11
Physikalisch-Technische Bundesanstalt
Abbestr. 2-12
10587 Berlin
Phone: (+49)-30-3481-7632
Fax: (+49)-30-3481-7505
email: wolfgang.kilian@ptb.de

Abstract

Hyperpolarized ^{129}Xe (HpXe) NMR not only holds promise for functional lung imaging but for measurements of tissue perfusion as well. To investigate human brain perfusion, several time-series of ^{129}Xe MR spectra were recorded from one healthy volunteer after HpXe inhalation. The time-dependent amplitudes of the MR spectra were analyzed by using a compartment model for xenon uptake modified to account for the loss of ^{129}Xe polarization due to RF-excitation and for the breath-hold technique used in the experiments. This analysis suggests that the resonances detected at 196.5 ± 1 ppm and 193 ± 1 ppm originate from HpXe dissolved in grey and white matter, respectively, and that T_1 relaxation times of HpXe are different in grey and white matter ($T_{1_g} > T_{1_w}$).

INTRODUCTION

When hyperpolarized ^{129}Xe (HpXe) MRI was demonstrated initially in 1994 (1), the feasibility of air space imaging using laser-polarized noble gases was shown, and of particular interest to our studies, the potential for tissue-perfusion studies with dissolved HpXe was outlined. The basic model of inert gas exchange in the lungs and in tissues was developed by Kety (2). Here, the accurate determination of brain perfusion was one of the most challenging issues. Initially the arteriovenous gas-concentration difference was determined by taking blood samples (3). More direct measurement of brain perfusion was possible by monitoring the accumulation of radioactive ^{133}Xe in brain tissue (4). To improve spatial resolution, xenon-enhanced CT (5) has been used during the last 20 years. Nevertheless, the relatively high concentration of Xe in the inhaled gas (35 % Xe gas over ≈ 10 min) needed for Xe CT can cause adverse physiological effects, especially in patients (6). In contrast, HpXe MR may yield high spatial and temporal resolution without such disadvantageous side effects.

To assess the potential of HpXe cerebral MRI several theoretical models have been developed (7–9). In general there are two ways to administer HpXe for perfusion measurements: inhalation of HpXe gas or injection of a lipid emulsion containing dissolved HpXe. In reference (9) it was concluded that respiration and intravenous injection lead to comparable concentrations of HpXe in the brain. Intraarterial injection, which results in higher HpXe concentrations in the corresponding tissue, is highly invasive (10). Therefore, a breath-hold technique after inhaling ≈ 0.5 liter HpXe gas is considered to be a safe and easily implemented alternative for human MR brain studies, first demonstrated in (11).

In this paper we present a compartment model (7) adapted to the breath-hold technique used in our experiments and intended to account for the destruction of polarization by repetitive RF excitations. To validate the model and to demonstrate the clinical feasibility of HpXe MR brain perfusion studies, we performed spectroscopic MR measurements at various times after inhaling HpXe gas and determined the time-dependent Xe concentration within the brain. To our knowledge we report the first quantitative human *in vivo* brain perfusion studies using HpXe.

^{129}Xe UPTAKE MODEL

We modified the model described in (7), which assumes a constant inhalation of HpXe, for the breath-hold technique used in our experiments. We additionally assumed that the HpXe gas is contained in the

Table 1: Model parameters taken from reference (7) unless stated otherwise

compartments	Xe solubility coefficients	pulm. blood flow $\dot{Q}$; perfusion rates F_i	longitudinal relaxation times
lung alveoli		$\dot{Q} = 83\,\mathrm{cm}^3/\mathrm{s}$	$T_{1_A} = 16\,\mathrm{s}$
arterial blood	$\lambda_B = 0.17$		$T_{1_B} = 6.4\,\mathrm{s}$ (12)
grey matter	$\lambda_g = 0.135$	$F_g = 0.80\,\mathrm{min}^{-1}$	$T_{1_{brain}} = 14\,\mathrm{s}$ (13) *
white matter	$\lambda_w = 0.224$	$F_w = 0.21\,\mathrm{min}^{-1}$	$T_{1_w} = 8\,\mathrm{s}$ **

*taken as T_{1_g} in this paper; ** derived in this study

alveolar volume V_A (≈ 3 liter) instantaneously at the beginning of the experiment ($t = 0$). The resulting initial alveolar concentration of HpXe gas is $C_A(t=0) \equiv C_{A,0} = n_{^{129}Xe} P_{Xe}/V_A$ where $n_{^{129}Xe}$ is the number of moles of ^{129}Xe gas inhaled ($n_{^{129}Xe} \approx 5.3$ mmol for ≈ 0.5 liter HpXe gas of natural abundance [26 % ^{129}Xe] inhaled at room temperature and atmospheric pressure) and P_{Xe} is the initial polarization. After inhalation of HpXe, pulmonary blood is rapidly saturated (e.g. within 70 ms as measured in a dog (14)) with HpXe. Its concentration in blood is determined by the Ostwald solubility coefficient λ_B which is the ratio of the volume of dissolved gas per unit volume of solvent (blood) at equilibrium. The time required to saturate the blood is short compared to all other times involved and, therefore, was neglected. Assuming that the transit times of blood through capillaries can also be neglected, the concentration C_A of HpXe within the alveoli depends on the longitudinal relaxation time T_{1_A} within the alveoli and on the uptake of HpXe by blood with a pulmonary blood flow $\dot{Q}$

$$C_A(t) = C_{A,0}\, e^{-t\left(1/T_{1_A} + \lambda_B \dot{Q}/V_A\right)}\,. \qquad [1]$$

The HpXe concentration $C_B(t)$ in arterial blood reaching the tissue of interest (brain) at time t is determined by the Ostwald solubility factor λ_B times the alveolar HpXe concentration $C_A(t - t_B)$, where $t_B \approx 4$ s is the time required for the blood to reach the brain capillaries. Correcting for the relaxation of HpXe in arterial blood at the rate $1/T_{1_B}$ during the time t_B, one obtains

$$C_B(t) = \lambda_B\, C_A(t - t_B)\, e^{-t_B/T_{1_B}}\,. \qquad [2]$$

Following the Kety model (2) one derives from Fick's principle the change of HpXe concentration within the tissue to be

$$\frac{d\,C_i(t)}{dt} = F_i \left(C_B(t) - \frac{1}{p_{iB}} C_i(t) \right) - \frac{C_i(t)}{T_{1_i}}\,, \qquad [3]$$

where F_i is the perfusion rate (measured in milliliters of blood per milliliter of tissue per minute) and $p_{iB} = \lambda_i/\lambda_B$ is the partition coefficient between the tissue i (including the blood contained in it) with an Ostwald solubility coefficient λ_i and blood. The last term in Eq. [3] was included to account for the decay of polarization in the tissue at the rate $1/T_{1_i}$. Using Eqs. [1] and [2], one can solve Eq. [3] for the initial conditions $C_{i,0}(t_B) \equiv 0$ and $C_{i,n}(t_B + n\Delta t) \equiv \cos\alpha \cdot C_{i,n-1}(t_B + n\Delta t)$ $[n \geq 1]$ to account for the destruction of polarization within the tissue i by n RF excitations (separated by Δt) at a flip angle α. One

obtains for the time-dependent HpXe concentration $C_{i,n}(t)$ after the n-th RF excitation in tissue i:

$$C_{i,n}(t) = \frac{\delta_i}{\beta_i - \gamma}\left(e^{-\gamma(t-t_B)} - e^{-\beta_i(t-t_B)}\eta_{i,n}\right) \quad [4]$$
$$\text{for} \qquad t_B + n\Delta t \le t \le t_B + (n+1)\,\Delta t$$

with

$$\begin{aligned}
\beta_i &= \tfrac{F_i}{p_{iB}} + \tfrac{1}{T_{1_i}} \\
\gamma &= \tfrac{1}{T_{1_A}} + \tfrac{\lambda_B \dot{Q}}{V_A} \\
\delta_i &= F_i \lambda_B C_{A,0}\, e^{-t_B/T_{1_B}} \\
\eta_{i,0} &= 1 \\
\eta_{i,n} &= (1-\cos\alpha)\; e^{-(\gamma-\beta_i)n\Delta t} + \eta_{i,n-1}\cos\alpha\,.
\end{aligned}$$

In Eq. [4], the first term describes the diminishing uptake of HpXe by the tissue from the arterial blood, while the second term accounts for washout and relaxation processes. For $\alpha = 0$, all $\eta_{i,n} = 1$, yielding a smooth variation of the HpXe concentration $C_i(t)$ with time. Furthermore, if $\beta_i = \gamma$, i.e. wash-in and wash-out rates are equal, all $\eta_{i,n} = 1$ and hence destruction of polarization by RF pulses does not affect $C_i(t)$. Equation [4] was used to calculate time-dependent concentrations (C_g, C_w) of HpXe dissolved in grey and white matter (Fig. 1), using the parameters listed in Tab. 1. The downward steps in the HpXe concentration represent the destruction of polarization by the RF excitations. Experimentally measured MR signal amplitudes would be proportional to the concentrations just before each step. To illustrate the influence of the various relaxation times in Fig. 1, C_g was calculated for various values of T_{1_g}, keeping T_{1_A} fixed at 16 s, whereas C_w was evaluated for various values of T_{1_A} at a fixed $T_{1_w} = 8\,\text{s}$. Since $T_{1_A}^{-1} \gg \frac{\lambda_B \dot{Q}}{V_A}$ and $C_i(t) \approx \frac{\delta_i}{\beta_i - \gamma} e^{-\gamma(t-t_B)}$ (for $\alpha = 0$, $(t-t_B)\,(\beta_i - \gamma) \gg 1$), a change in T_{1_A} directly effects the falling slope of the concentration C_i whereas a change in T_{1_i} results in a parallel shift of the falling slope of C_i, caused by the factor $(\beta_i - \gamma)^{-1}$. It should be noted that the ratio C_g/C_w is determined essentially by the ratio of the perfusion rates of grey and white matter.

MATERIALS AND METHODS

Production of HpXe Gas

Hyperpolarized ^{129}Xe was produced by spin-exchange optical pumping (15) using a home-built apparatus (16). Circularly-polarized light from three high-power laser diode arrays (COHERENT, Dieburg,

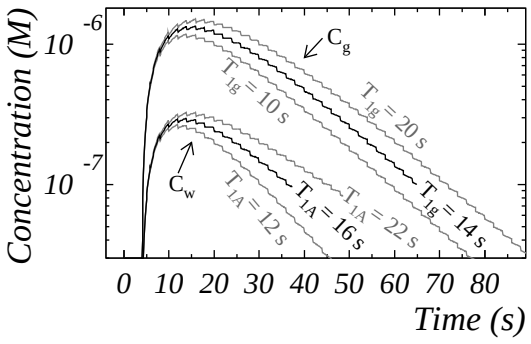

Figure 1: Theoretical concentrations (C_g, C_w) of HpXe in grey and white matter calculated with Eq. 4 by using the parameter values given in Tab. 1 (unless shown otherwise) and $P_{Xe} = 15\%$, $\alpha = 20^{\text{o}}$ and $\Delta t = 2\,\text{s}$.

Germany, FAP-I, 30 W) was directed from both sides into the heated cylindrical pumping cell (V_{cell} = 70 ccm, $T_{cell} \approx 180\,^{o}$C) to excite the D_1-line of Rb-vapor produced from a droplet of Rb in the cell. The electron spin polarization of Rb was transferred to the ^{129}Xe nuclear spin by collisional spin-exchange. A gas mixture of 2 % Xe (natural abundance), 4 % N_2 and 94 % ^{4}He at a total pressure of 5 bar was passed through the optical pumping cell at a steady rate of 403.6 ml_n/min (**?**), and subsequently through a cold trap at liquid N_2 temperature, situated in a magnetic field of $\approx$ 70 mT, to separate the HpXe from the remaining gases. After one hour of optical pumping the accumulated HpXe ice was quickly evaporated into a Tedlar^{TM} (plastic) bag. In this way about 0.5 liter of HpXe at atmospheric pressure was produced with ^{129}Xe polarizations ranging from 8 to 15 %. The remaining HpXe gas in the cold trap was further expanded into an evacuated detachable glass bulb (5 cm diam.) and used to determine the absolute polarization P_{Xe} by NMR calibration measurements.

NMR Methods

All MR measurements were carried out on a MedSpec 30100 scanner (BRUKER BIOSPIN MRI, Ettlingen, Germany) at a field strength of 2.94 T by using a 10 cm diameter transmit-receive surface coil tuned to the ^{129}Xe resonance frequency (34.7 MHz). A Gaussian excitation pulse of 1 ms duration was applied to record free induction decays (FIDs) without any spatial encoding.

In order to measure P_{Xe} of the HpXe gas used in each session, the MR signal was recorded from the detachable glass bulb filled with HpXe at known pressure and compared with the signal obtained from thermally polarized ^{129}Xe gas. This procedure gave the polarization P_{Xe} of the HpXe to within 15% of the actual value.

By using the 5 cm glass bulb filled with HpXe gas, the flip angle α applied in the *in vivo* measurements was estimated by recording trains of 20 FIDs (RF pulse repetition time $\Delta t = 3s$), where each train had a different transmitter power setting. For this purpose the transmit-receive coil was placed on a tissue equivalent phantom, simulating the loading of the coil by the head as deduced from Q-factor measurements. The glass bulb was positioned two centimeters above the surface coil, covering the region where signals from the volunteer's head had been measured with a 1D-CSI sequence (no signals from the scalp were seen (17)). Although the B_1 field of a 10 cm diameter surface coil is strongly inhomogeneous over the volume of the human head, average flip angles α_{est} were estimated by fitting the amplitudes from a given train of FIDs to $\cos^n \alpha_{est}$.

Protocol for *in vivo* Investigations

Measurements were performed on one healthy volunteer (one of the authors, WK) lying in the prone position with the back of his head resting on the surface coil, resulting in a detection volume with nearly equal amounts of grey and white matter. Heart rate and blood oxygenation were monitored with a pulse oximeter (M3500, MAGNETIC RESONANCE EQUIPMENT CORPORATION, Washington, USA). In each of five separate experiments (sessions) a train of n ^{129}Xe FIDs was recorded at different flip angles α, RF pulse repetition times Δt and initial ^{129}Xe polarizations P_{Xe} (see Table 2). The excitation pulse was tuned to 200 ppm with respect to the ^{129}Xe gas resonance frequency and FIDs were acquired at a bandwidth of 20 kHz, sampling 2048 complex data points. For data analysis each FID was multiplied by a Gaussian (σ = 700 data points) prior to applying a fast Fourier transform, resulting in a line broadening of about 28 Hz ($\approx$ 0.8 ppm). The first FID of a session was acquired with the Tedlar bag positioned beside the

Table 2: Parameters used in the five experiments (P_{Xe} for Exp. #1 was not measured).

Exp.	#1	#2	#3	#4	#5
α_{est}	28°	14°	28°	28°	56°
Δt	2 s	2 s	5 s	2 s	2 s
n	60	60	24	60	60
P_{Xe}	-	11 %	8 %	15 %	10 %

volunteer's head to record the gas reference signal. Subsequently the volunteer quickly inhaled 0.5 liter of HpXe gas followed by additional air and held his breath as long as possible (≈ 40 s). It follows from the results reported in (6) that xenon concentrations in the body achieved in this way are far below those at which serious side effects occur. As expected, no abnormal physiological sensations were noticed by the volunteer during and after HpXe inhalation.

RESULTS AND DISCUSSION

In each of the spectra that showed ^{129}Xe signals we observed a predominant line at 196.5 ± 1 ppm and a weaker signal at 193 ± 1 ppm. We did not see any signal at ≈ 215 ppm, which would have presumably originated from HpXe dissolved in blood, consistent with the small volume fraction (≈ 5 %) of blood within the brain (Fig. 2). In order to derive the amplitudes of the 196.5 ppm and 193 ppm lines, the sum of two Gaussian lineshapes was fitted to each spectrum. The center frequencies for these Gaussians were restricted to the chemical shift ranges $195\,\text{ppm} < \delta_0 < 198\,\text{ppm}$ and $192\,\text{ppm} < \delta_0 < 194\,\text{ppm}$. Both Gaussians were assumed to have the same width, which was restricted to the range $0.5\,\text{ppm} < \sigma < 1\,\text{ppm}$. In Fig. 2, the dashed line corresponds to the fitted line shape obtained in this way.

In the very first *in vivo* human brain studies (11) using HpXe, one predominant line was seen at 196 ppm with broadened shoulders on either side. This line was attributed to HpXe dissolved in brain parenchyma. More detailed information was obtained from animal (rat) studies. Chupp *et al.* (18) attributed the dominant line measured at 194.5 ppm (in rat brain spectra) to HpXe dissolved in grey matter and speculated that the signal at 189 ppm might arise from HpXe in white matter.

Likewise, we assumed that the dominant line we detected at 196.5 ppm originated from HpXe dissolved in grey matter. This assignment is supported by preliminary *in vivo* results obtained from 2D CSI of HpXe in human brain (17) where the highest signals from the dominant line occurred in regions

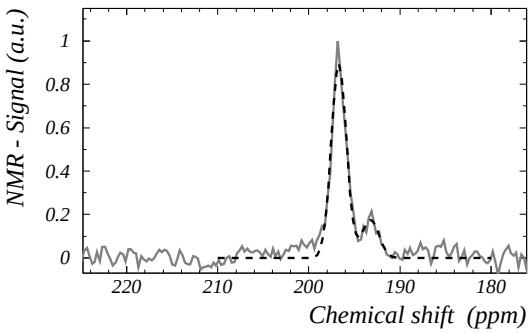

Figure 2: *In vivo* ^{129}Xe spectrum from experiment #4 (taken 18 s after HpXe inhalation) with a two-Gaussian fit (dashed line) for amplitude determination.

containing mainly grey matter. We then calculated time-dependent concentrations of HpXe dissolved in grey and white matter by using the model for ^{129}Xe uptake discussed above, the parameters specified in Tab. 1, and assuming $T_{1_g} = T_{1_w} = T_{1_{brain}}$. Subsequently, the dynamics of these predicted concentrations were compared to the dynamics of the measured amplitudes of the lines at 196.5 ppm and 193 ppm. For this purpose the signal amplitudes of all spectra recorded within the same experiment were scaled by the same factor. In addition, the data were shifted in time to match the maximum of the signal amplitude of the 196.5 ppm line with the maximum of the theoretical concentration curve of HpXe in grey matter. Comparison of the theoretical and experimental results suggested that the average flip angle α_{est}, determined by our phantom measurements, overestimated the actual value. In particular, this was noticeable for experiments taken at $\Delta t = 2$ s and larger RF amplitudes (Exp. #4, #5). By varying α and minimizing the sum of squared differences between the theoretical concentration of HpXe in grey matter and the scaled 196.5 ppm line amplitudes, we deduced the actual effective flip angle to be $\alpha_{\text{eff}} = 0.7\,\alpha_{\text{est}}$.

Fig. 3 compares scaled amplitudes of the lines at 196.5 ppm and 193 ppm derived from spectra of experiments #2 through #4 with time-dependent concentrations of HpXe in grey and white matter, respectively. Good agreement is seen between experimental data for the 196.5 ppm line and the theoretical concentrations C_g (solid lines). Although the use of effective flip angles affects the values for the relaxation times T_{1_g} and T_{1_w} needed to match experimental data and theoretical concentrations, our data could not be accounted for by using the same relaxation time ($T_{1_{brain}} = 14$ s (13)) for both the 196.5 ppm and 193 ppm lines, independent of the value chosen for α_{eff}. By minimizing the sum of squared differences and keeping α_{eff} fixed at $0.7\,\alpha_{\text{est}}$, good agreement between the theoretical concentration of HpXe in white matter C_w and the amplitudes of the 193 ppm line was obtained for a considerably shorter relaxation time, $T_{1_w} = 8$ s. Even when neglecting the destruction of polarization by repetitive RF-pulses (i.e. $\alpha = 0$, see dashed lines in Fig. 3), the values for the relaxation times $T_{1_g} = 14$ s and $T_{1_w} = 8$ s can account for our experimental data after rescaling. Furthermore, the ratio of the amplitude of the 196.5 ppm line to that for the 193 ppm line is well reproduced by the ratio C_g/C_w of the concentrations of HpXe in grey and white matter, calculated with physiological parameters of brain perfusion known from literature. This result, together with 1D-CSI measurements (17) showing intracranial signals only, strongly supports our assumption that the line at 193 ppm corresponds to HpXe dissolved in white matter.

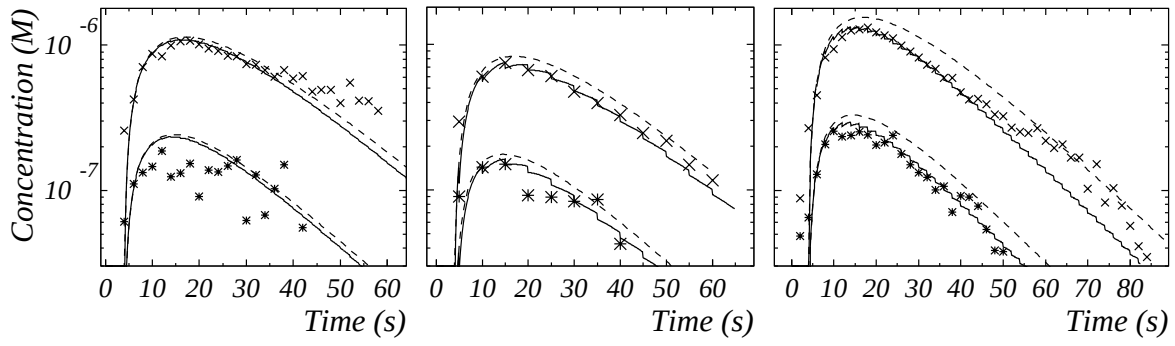

(a) Exp. #2: $\alpha_{\text{eff}} = 10°$, $\Delta t = 2$ s (b) Exp. #3: $\alpha_{\text{eff}} = 20°$, $\Delta t = 5$ s (c) Exp. #4: $\alpha_{\text{eff}} = 20°$, $\Delta t = 2$ s

Figure 3: Dynamics of the scaled amplitudes of the 196.5 ppm ($\times$) and 193 ppm ($*$) lines deduced from experiments #2 - #4, which used different acquisition parameters (see Tab. 2). The lines indicate theoretical concentrations calculated from Eq. 4 (fitting parameters: $T_{1_g} = 14$ s, $T_{1_w} = 8$ s; effective flip angles α_{eff} for solid lines and $\alpha = 0°$ for dashed lines).

CONCLUSION

We report for the first time on quantitative *in vivo* ^{129}Xe MR spectroscopy (MRS) in human brain using hyperpolarized xenon gas. Our results provide evidence that the two resonances at 196.5 ppm and 193 ppm originate from HpXe dissolved in grey and white matter, respectively. Furthermore we conclude that longitudinal ^{129}Xe relaxation in grey matter is slower than that in white matter ($T_{1_g} > T_{1_w}$). Although only one subject was investigated, our results are comparable to those of animal studies reported recently (13). Our measurement protocol turned out to be simple and robust. Our method should allow one to determine relative changes in the perfusion of various brain compartments, provided that concentrations of dissolved HpXe are sufficiently high to be detected by MRS, the various spectral lines observed can be assigned unambiguously to specific brain compartments, and their longitudinal relaxation times T_{1_i} can be measured with sufficient precision. Measurements of changes in perfusion between different compartments, obtained in this way, might be of diagnostic interest.

ACKNOWLEDGMENTS

We cordially thank Arno Villringer, M.D., for medical advice and supervision.

References

1. Albert MS, Cates GC, Driehuys B, Happer W, Saam B, Springer Jr CS, Wishnia A. Biological magnetic resonance imaging using laser-polarized ^{129}Xe. Nature 1994;370:199–201.

2. Kety SS. The Theory and Applications of the Exchange of Inert Gas at the Lungs and Tissues. Pharmacol Rev 1951;3:1–41.

3. Kety SS, Schmidt CF. The Determination of Cerebral Blood Flow in Man by the Use of Nitrous Oxide in Low Concentrations. Am J Physiol 1945;143:53–66.

4. Obrist WD, Thompson Jr HK, King CH, Wang HS. Determination of Regional Cerebral Blood Flow by Inhalation of 133-Xenon. Circulation Research 1967;20:124–135.

5. Drayer BP, Gur D, Wolfson Jr SK, Cook EE. Experimental Xenon Enhancement with CT Imaging: Cerebral Applications. Am J Radiol 1980;134:39–44.

6. Yonas H, Grundy B, Gur D, Shabason L, Wolfson Jr SK, Cook EE. Side Effects of Xenon Inhalation. J Comput Assist Tomogr 1981;5:591–592.

7. Peled S, Jolesz FA, Tseng CH, Nascimben L, Albert MS, Walsworth RL. Determinants of Tissue Delivery for ^{129}Xe Magnetic Resonance in Humans. Magn Reson Med 1996;36:340–344.

8. Martin CC, Williams RF, Gao JH, Nickerson LDH, Xiong J, Fox PT. The Pharmacokinetics of Hyperpolarized Xenon: Implications for Cerebral MRI. J Mag Res Imag 1997;7:848–854.

9. Lavini C, Payne GS, Leach MO, Bifone A. Intravenous delivery of hyperpolarized ^{129}Xe: a compartmental model. NMR Biomed 2000;13:238–244.

10. Duhamel G, Choquet P, Grillon E, Lamalle L, Leviel JL, Ziegler A, Constantinesco A. Xenon-129 MR Imaging and Spectroscopy of Rat Brain Using Arterial Delivery of Hyperpolarized Xenon in a Lipid Emulsion. Magn Reson Med 2001;46:208–212.

11. Mugler III JP, Driehuys B, Brookeman JR, Cates GD, Berr SS, Bryant RG, Daniel TM, de Lange EE, Downs III JH, Erickson CJ, Happer W, Hinton DP, Kassel NF, Maier T, Phillips CD, Saam BT, Sauer KL, Wagshul ME. MR Imaging and Spectroscopy Using Hyperpolarized ^{129}Xe Gas: Preliminary Human Results. Magn Reson Med 1997;37:809–815.

12. Wolber J, Cherubini A, Dzik-Jurasz ASK, Leach MO, Bifone A. Spin-lattice relaxation of laser-polarized xenon in human blood. Proc Natl Acad Sci 1999;96:3664–3669.

13. Duhamel G, Choquet P, Grillon E, Leviel JL, Ziegler A, Constantinesco A. Brain perfusion measurement using hyperpolarized xenon-129 MRI. In: Proc 10th ISMRM Scientific Meeeting, Honolulu, 2002. p 1092.

14. Ruppert K, Brookeman JR, Hagspiel KD, Driehuys B, Mugler III JP. NMR of hyperpolarized ^{129}Xe in the canine chest: spectral dynamics during a breath-hold. NMR Biomed 2000;13:220–228.

15. Walker T, Happer W. Spin-exchange optical pumping of noble-gas nuclei. Rev Mod Phys 1997;69:629–642.

16. Kilian W. Erzeugung von hyperpolarisiertem ^{129}Xe-Gas und Nachweis mittels in vivo NMR-Bildgebung, NMR-Spektroskopie sowie SQUID-Messtechnik. PhD thesis;Freie Universität Berlin;2001. www.diss.fu-berlin.de/2001/105/.

17. Kilian W, Seifert F, Rinneberg H. Chemical Shift Imaging of Human Brain after Inhaling Hyperpolarized ^{129}Xe-Gas. In: Proc. Intl. Soc. Mag. Reson. Med. 10;Honolulu. 2002. p 758.

18. Chupp TE, Coulter KP, Rosen MS, Swanson SD. Chemical shift imaging of laser-polarized ^{129}Xe magnetization in rats in vivo. Eur Radiol 1999;9:B45. Int. workshop, Les Houches, June 21-25, 1999.